Explicit Motion Compensation for Backprojection in Spotlight SAR

Aron Sommer
Institut für Informationsverarbeitung
Leibniz Universität Hannover
Hannover, Germany
sommer@tnt.uni-hannover.de

Jörn Ostermann
Institut für Informationsverarbeitung
Leibniz Universität Hannover
Hannover, Germany
office@tnt.uni-hannover.de

***Abstract*—In an airborne Synthetic Aperture Radar (SAR) scenario, the global Backprojection algorithm enables processing of non-linear flight paths, but not with variable velocities of the aircraft. The proposed additional explicit motion compensation uses an equidistant resampling of the flight path to ensure high image quality, despite variable platform velocity (even negative velocities) and flight paths including loops. Hence, small helicopters or minicopters could be used for SAR. Numerical simulations show the capability of the proposed algorithm, even for motion errors greater than 50 m.**

I. Introduction

Standard Synthetic Aperture Radar (SAR) systems assume that the platform moves with constant velocity along a linear path [2]. Especially in the airborne case, atmospheric turbulences cause deviations from the nominal flight path. These displacements lead to a loss of quality in the focused image. Small motion errors up to approximately 10 m [9] can be emended by motion compensation techniques developed for frequency domain algorithms. Greater deviations can only be compensated by time domain algorithms like global Backprojection [5]. Their implicit motion compensation corrects arbitrary flight paths. However, even when using global Backprojection respected large velocity variations yield smeared images.

In the past some motion compensation techniques [3], [4], [6], [7] were developed for frequency domain algorithms to compensate deviations from the nominal straight line. Motion compensation techniques of higher order [3], [4], [8] reduce quality loss for large illuminated areas. All of these algorithms consider small deviations and small velocity changes. In this paper, we consider extreme deviations to a straight line like loops and oscillations up to 50 m, like a helicopter can fly.

We show that motion compensation techniques can be used to compensate non constant velocities of the platform, even for negative velocities.

This paper is structured as follows. In Section II we present the signal model which is used to generate synthetic data. The proposed algorithm, including the resampling process and the motion compensation technique, is shown in Section III. An X-band SAR system is simulated in Section IV which presents the quality gain using the proposed algorithm. Section V concludes this paper.

II. Signal Model

Consider an airplane which moves with non-constant velocity v along an arbitrary flight path $\boldsymbol{\gamma} : \mathcal{L} \to \mathbb{R}^3$ within the synthetic aperture time $s \in \mathcal{L} := [0, T_a]$. During the illumination process, the radar sends electromagnetic chirp pulses

$$p(t) = \text{rect}(\tfrac{t}{T}) \exp(2\pi i f_c t) \exp(i\pi\kappa t^2), \qquad t \in \mathcal{T},$$

with fast time t, carrier frequency f_c, chirp rate κ, pulse duration T, speed of light c and sampling time interval $\mathcal{T}$. After these pulses are scattered at the ground, which we assume to be an xy-plane at height $z = 0$, they travel back to the antenna. For example one point-like scatterer located at x_p, see Figure 1, causes the range compressed data

$$d_{\boldsymbol{x}_p}(t, s) = \text{si}\left(\pi\kappa T\Big(t - \tfrac{2||\boldsymbol{\gamma}(s) - \boldsymbol{x}_p||_2}{c}\Big)\right) \cdot \exp\Big(-2\pi i f_c \tfrac{2||\boldsymbol{\gamma}(s) - \boldsymbol{x}_p||_2}{c}\Big).$$

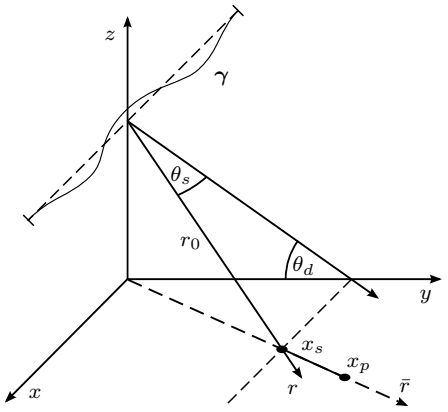

Fig. 1. Squinted spotlight SAR geometry, where $\boldsymbol{\gamma}$ is the actual flight path, x_s the spot center, θ_s the squint angle and θ_d the depression angle. We choose the distance from the flight path center to x_s to be $r_0 = 16$ km and place a point target 1 km away from x_s along ground range $\bar{r}$.

Superposition of all scatterers inside the whole scene yields the signal model of the received and range compressed signal

$$d(t,s) = \int_{\Omega} A(t,s,\boldsymbol{x})\,\mathcal{V}(\boldsymbol{x})\ \mathrm{si}\left(\pi\kappa T\Big(t - \tfrac{2||\boldsymbol{\gamma}(s)-\boldsymbol{x}||_2}{c}\Big)\right) \cdot \exp\left(-2\pi i f_c \tfrac{2||\boldsymbol{\gamma}(s)-\boldsymbol{x}||_2}{c}\right) \mathrm{d}\boldsymbol{x}, \quad (1)$$

given by Cheney [1], where A is the antenna beam pattern and Ω the illuminated scene. The reflectivity function $\mathcal{V}$ represents the scene, more precisely the reflectivity of the scattered objects.
Note that in a spotlight scenario the antenna beam pattern A can be neglected, because all targets are within the area Ω.

III. Explicite Motion Compensation

In general, common motion compensation techniques [3], [4], [6], [7] assume the knowledge of the actual flight path, accurately measured by an inertial navigation system (INS) and a global positioning system (GPS).

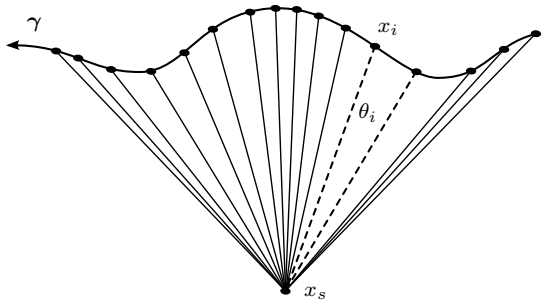

Fig. 2. Actual flight path sampled with constant pulse repetition frequency. The variable velocity of the platform results in non equidistant sampling of the incident angle θ_i, which is illustrated by lines between the aperture positions x_i and the spot center x_s.

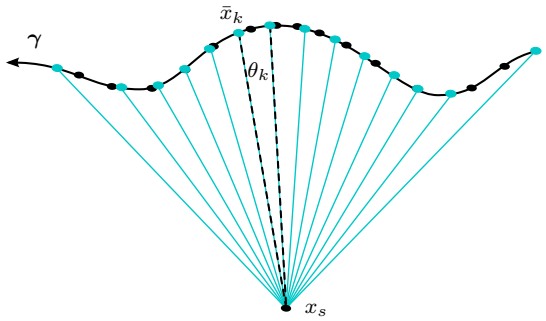

Fig. 3. Resampled flight path with equidistant sampled incident angles θ_i, which is illustrated by lines between the new aperture positions $\bar{x}_k$ and the spot center x_s.

These techniques use the known deviation from the nominal straight line to manipulate the range compressed data so that the corrected data fits to the nominal flight path. In our scenario this standard technique cannot be used, because these deviations to the straight flight path are too large. In contrast, we choose the nominal flight path to be the resampled actual flight path, not a straight line. We resample the real flight path, so that the new aperture positions along the actual path have equidistant incident angles, see Figure 2 and 3. Secondly, motion compensation changes the raw data to fit to the resampled aperture positions on the flight path, see Figure 4. Special adjustments to the Backprojection algorithm are not necessary. Subsequently, the algorithm is described in detail:

1) Flight Path Resampling: The main cause of the loss of image quality using Backprojection is the non equidistant slow-time sampling in azimuth produced by accelerations of the airplane or turbulences in azimuth, see Figure 2. To overcome this effect, we introduce new aperture positions $\bar{x}_k$ along the flight path, so that all angles θ_i are equal, see Figure 3.

2) Explicit Motion Compensation: After resampling the flight path, the range compressed data d, measured at the old aperture positions x_i, has to be compensated to match the new aperture positions $\bar{x}_k$. For the motion compensation we choose the factorization process of the Fast Factorized Backprojection algorithm [10], because the resampling and interpolation of the range compressed data can be performed for arbitrary trajectories easily. It follows the same basic idea of other first order motion compensation methods of frequency domain algorithms and works in the following way:
Firstly, for every new aperture position $\bar{x}_k$ the nearest old aperture position x_i has to be found by

$$x_i = \underset{l}{\mathrm{argmin}} ||\bar{x}_k - x_l||_2.$$

Moreover, for every fast-time sample t_j, $j = 1,\ldots,n$, transferred to range $r_j = \frac{c}{2}t_j$, the range difference $r_j - r_{i,j}$ is needed. This distance can be computed easily in polar coordinates using the law of cosines. In that manner the angle ϑ_k between the direction of view $\vec{r}_k := \bar{x}_k - x_s$ and the local flight direction $\vec{u}_{k,i} := \bar{x}_k - x_i$ is computed by

$$\cos\vartheta_k = \frac{\vec{r}_k^{\top} \cdot \vec{u}_{k,i}}{||\vec{r}_k||_2\,||\vec{u}_{k,i}||_2},$$

which brings us directly to the required distance

$$r_{i,j} = \sqrt{r_j + ||\vec{u}_{k,i}||_2 - 2\,r_j||\vec{u}_{k,i}||_2\cos\vartheta_k}.$$

This range difference $r_j - r_{i,j}$ is used to compute the motion compensated, range compressed data $\widetilde{d}$ by an interpolation plus phase correction to reduce the corrupted phase:

$$\widetilde{d}(\bar{s}_k, r_j) = d(s_i, r_{i,j}) \cdot \exp\left(\tfrac{4\pi i f_c (r_j - r_{i,j})}{c}\right). \quad (2)$$

The slow-time $\bar{s}_k$ belongs to the aperture position $\bar{x}_k$.

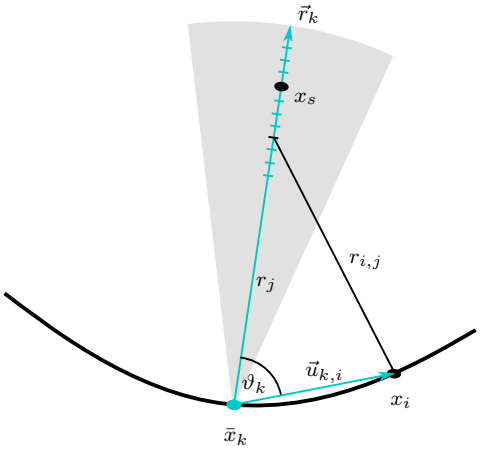

Fig. 4. Concept of phase error calculation of the motion compensation method. Here x_i is the old aperture position, $\bar{x}_k$ the new aperture position, x_s the spot center and $\vec{r}_k$ the current line of sight.

3) Backprojection: After the motion compensation in form of a preprocessing step has finished, the time domain image formation procedure can be done without any adjustments. Here we use the global Backprojection algorithm

$$I(\boldsymbol{x}) = \int_{\mathcal{L}} d\Big(\tfrac{2||\boldsymbol{\gamma}(s)-\boldsymbol{x}||_2}{c}, s\Big) \cdot \exp\Big(2\pi i f_c \tfrac{2||\boldsymbol{\gamma}(s)-\boldsymbol{x}||_2}{c}\Big)\, \mathrm{d}s$$

based on Gorham's implementation [5]. However, the Fast Factorized Backprojection algorithm can also be used to save computational costs.

In summary, the proposed explicit motion compensation for Backprojection shows its strength in such cases where huge deviations from the straight line, like loops, have to be compensated. Since its motion compensation technique is based on the factorization process of the Fast Factorized Backprojection algorithm [10], the approximated phase in equation (2) leads to small range errors. Despite these difficulties, the proposed algorithm yields good image quality when dealing with large variations of the platform speed. Nevertheless, if only small accelerations of the platform are present, the global Backprojection algorithm without the explicit motion compensation results acceptable image quality.

IV. Simulation Results

Based on one example, we show the improvement of the image quality using the proposed explicit motion compensation technique.

We simulate an X-band SAR system with parameters listed in Table I. The illuminated spot consists of one point reflector placed 1 km away from the spot center, see Figure 1. This demonstrates the independence of the image quality from range scene size, in contrast to frequency based algorithms [9]. The spot center is $r_0 = 16$ km away from the flight path.

TABLE I
Parameters of simulated X-band SAR system.

Parameter	Value
Carrier frequency f_c	9.6 GHz
Pulse bandwidth B	300 MHz
Pulse duration T	6 μs
Sampling frequency f_s	350 MHz
Platform velocity v_0	100 m/s
Synthetic aperture length L	400 m
Pulse repetition frequency prf	500 Hz
Synthetic aperture time T_a	4 s
Squint angle θ_S	10°
Depression angle θ_D	25°

The actual flight path $\boldsymbol{\gamma}$ is modeled by superposition of a straight line $\overline{\boldsymbol{\gamma}}$ and some oscillations $\widetilde{\boldsymbol{\gamma}}$:

$$\boldsymbol{\gamma}(s) = \overline{\boldsymbol{\gamma}}(s) + \widetilde{\boldsymbol{\gamma}}(s), \qquad s \in \mathcal{L}\,.$$

The curvy summand $\widetilde{\boldsymbol{\gamma}}$ is generated by a 3D colored noise function, in detail by additive Gaussian white noise, lowpass-filtered by a Hann window in x, y and z. Thus, the behavior of $\boldsymbol{\gamma}$ can be described by the variance σ^2 of $\widetilde{\boldsymbol{\gamma}}$.

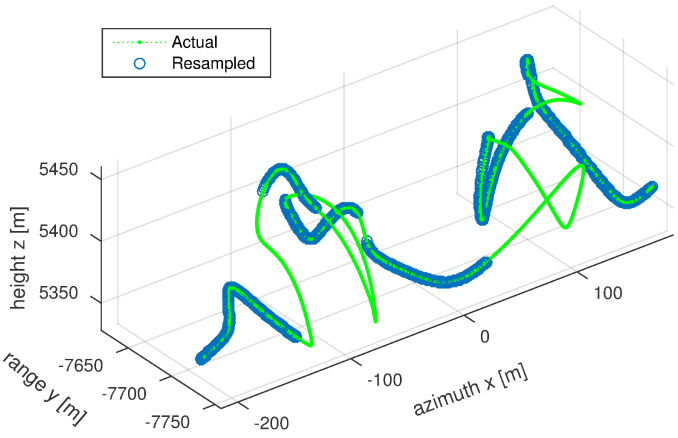

Fig. 5. Actual flight path with a variance of 20 m illustrated by the thin, green line. The resampling of the flight path in azimuth yields to the bold, blue line segments. The thin, green flight path leads to the results in Figure 6. The bold, blue flight path results to Figure 7.

Using a standard deviation of $\sigma = 20$ m simulates a flight path $\boldsymbol{\gamma}$ shown in Figure 5. Especially the large deviations in azimuth lead to negative velocities and therefore to the extreme course.

Applying the global Backprojection algorithm to the range compressed data d generated by equation (1) yields the results in Figure 6. It presents the processed image without the proposed motion compensation, whereas in Figure 7 the explicit motion compensation is used.

The results show that the non-equidistant sampling in azimuth of the actual flight path, see Figure 2, negatively impacts the image quality.

As image quality functions we use the 1D integrated side lobe ratio (ISLR) [11] and the 1D peak side lobe ratio (PSLR) [11],

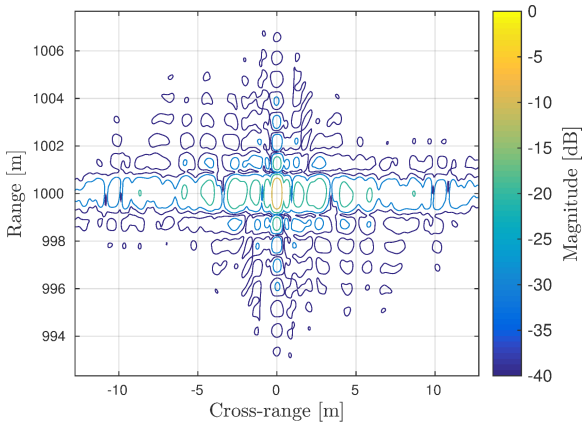

Fig. 6. Image of point reflector processed by global Backprojection. The actual flight path, shown as the thin, green line in Fiugre 5, is used.

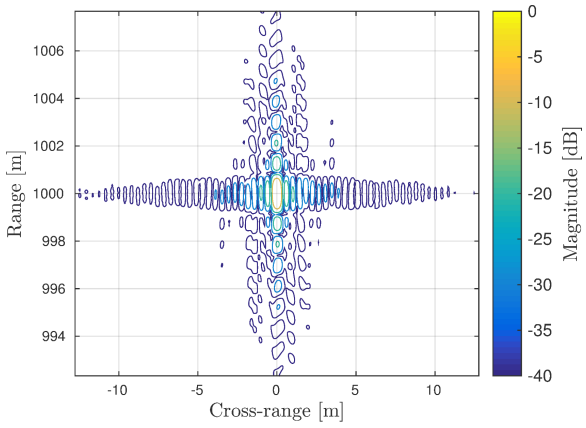

Fig. 7. Image of point reflector processed by global Backprojection. The proposed explicit motion compensation is applied, so that the resampled flight path, shown as the bold, blue line in Fiugre 5, is used.

both along azimuth to verify the results. The ISLR is calculated by

$$\text{ISLR} = 10\log_{10}\left(\frac{P(-20\,\delta_{az},-\delta_{az})+P(\delta_{az},20\,\delta_{az})}{P(-\delta_{az},\delta_{az})}\right),$$

where

$$P(a,b) = \int_a^b |I(x,y)|^2 \mathrm{d}x$$

is the power of the image intensity I. The range cell with maximal energy is denoted by , y and the spatial resolution in azimuth by δ_{az}. The PSLR is computed by

$$\text{PSLR} = 10\,\log_{10}\frac{I_s}{I_m}.$$

Here I_s is the peak intensity of the side lobe and I_m the peak intensity of the main lobe. We use no window function for side lobe suppression.

Our algorithm emended the image quality up to an azimuthal ISLR of -9.69 dB, see Table II. The point reflector in Figure 7 is not perfectly focused in range, because the extreme deviations in y and z, as well as the long aperture, causes range errors in the phase correction process described in equation (2). The deterioration of the image along azimuth is expressed in Table II in terms of ISLR and PSLR.

TABLE II
AZIMUTHAL IMAGE QUALITY OF A POINT REFLECTOR

	ISLR	PSLR
Standard Backprojection (Fig. 6)	-1.19 dB	-10.78 dB
Motion compensation Backprojection (Fig. 7)	-9.69 dB	-13.24 dB

V. CONCLUSION

The global Backprojection algorithm compensates motion errors regarding deviations from a nominal linear flight path. Especially big changes of the velocity result in a non equidistant sampling of aperture positions in azimuth, which yields a loss of image quality.

The new resampling of the flight path ensures high image quality. In total, the proposed explicit motion compensation technique for Backprojection enables the processing of SAR data, measured along a highly non linear flight path, flown, for example, by a helicopter.

REFERENCES

[1] M. Cheney, B. Borden, *Fundamentals of Radar Imaging*, SIAM, Philadelphia, 2009.

[2] I. A. Cumming, F. H. Wong, *Digital Processing of Synthetic Aperture Radar Data - Algorithms and Implementation*, 1-th edition, Artech House, Boston, 2005.

[3] G. Fornaro, *Trajectory Deviations in Airborne SAR: Analysis and Compensation*, IEEE Transaction on Aerospace and Electronic Systems, pp. 997-1009, July 1999.

[4] G. Fornaro, G. Franceschetti and S. Perna, *Motion Compensation of Squinted Airborne SAR Raw Data: Role of Processing Geometry*, Proc. of IEEE IGARSS 04, vol. 2, pp. 15181521, September 2004.

[5] L. A. Gorham, L. J. Moore, "SAR image formation toolbox for MATLAB", Proc. SPIE, Vol. 7699, Algorithms for Synthetic Aperture Radar Imagery XVII, 2010.

[6] H. Klausing and W. Holpp, *Radar mit realer und synthetischer Apertur*, Oldenbourg Verlag Mnchen, Wien, 2000.

[7] M. P. Nguyen, *Refined Motion Compensation for Highly Squinted Spotlight Synthetic Aperture Radar*, pp. 738–741, 2012.

[8] M. P. Nguyen, S. B. Ammar, *Second Order Motion Compensation for Squinted Spotlight Synthetic Aperture Radar*, Proc. APSAR 2013, pp. 202–205, Tsukuba, 2013.

[9] A. Sommer, M. P. Nguyen, J. Ostermann, *Comparison of Omega-K and Backprojection regarding Spatial Resolution for Squinted Spotlight SAR with Motion Errors*, Proc. APSAR 2015, pp. 143–147, Singapore, 2015.

[10] L. M. H. Ulander, H. Hellsten and G. Stenstrm, *Synthetic-aperture radar processing using fast factorised back-projection*, IEEE Transactions on Aerospace and Electronic Systems, vol. 39, pp. 760776, July 2003.

[11] X. Lu, H. Sun, *Parameter assessment for SAR image quality evaluation system*, in Proceedings 1st Asian and Pacific Conference Synthetic Aperture Radar, pp. 58–60, Huangshan, 2007.